

MEASUREMENT OF HYDROXYL RADICAL DURING SUPPRESSION OF LOW PRESSURE OPPOSED FLOW METHANE/AIR DIFFUSION FLAMES BY $\text{Fe}(\text{CO})_5$, CF_3Br , AND N_2

R. R. Skaggs, K. L. McNesby,
R. G. Daniel, B. Homan, and A. W. Miziolek
U.S. Army Research Laboratory
Aberdeen Proving Ground, MD 21005

ABSTRACT

Laser-induced fluorescence and emission spectroscopy are used to measure hydroxyl radical (OH) in reduced pressure, non-premixed, opposed flow CH_4/air flames suppressed by N_2 , CF_3Br , and $\text{Fe}(\text{CO})_5$. For the flames studied, the decrease in OH concentration is found to be proportional to the amount of suppressant added. Suppression by $\text{Fe}(\text{CO})_5$ is shown to affect flame temperatures to a greater extent than suppression by N_2 or CF_3Br .

INTRODUCTION

Fires that occur in non-traditional environments such as aboard combat vehicles, inside aircraft hangers, or on board the space shuttle are usually extinguished using Halon 1301 (CF_3Br) or Halon 1211 (CF_2ClBr). These halogenated hydrocarbons have been implicated as contributing to stratospheric ozone destruction.* In compliance with international agreement, production of Halon 1301 and Halon 1211 has ceased, and current research is focused on finding alternative fire suppressant agents.

Besides these halogenated hydrocarbons, there are several chemicals, e.g., iron pentacarbonyl ($\text{Fe}(\text{CO})_5$), that are very effective flame suppressants. In fact, $\text{Fe}(\text{CO})_5$ may be one of the most effective inhibiting agents ever discovered [1,2,3], but the agent cannot be used in spaces occupied by personnel because it is highly toxic [4]. Even though $\text{Fe}(\text{CO})_5$ cannot be considered as a viable replacement for halon, understanding the mechanism responsible for its superior suppressant effectiveness might provide a path to identifying new fire suppressant agents.

BACKGROUND

Flame suppression by metal-containing compounds, such as $\text{Fe}(\text{CO})_5$, is assumed to proceed by either a gas phase (homogeneous) or gas-solid (heterogeneous) reaction mechanism [5]. In the homogeneous reaction mechanism, metal-oxygen monomers (or low molecular weight polymers) are formed and are collision participants in catalytic free radical removal and/or recombination mechanisms. For the heterogeneous reaction mechanism, metal-containing particles are formed and free-radical recombination reactions occur on the particle surface.

* Fourth Meeting of the parties to the Montreal Protocol on Substances that Deplete the Ozone layer, 23-25 Nov 1992, Copenhagen. Doc.no. UNEP/OzL.Pro.4/15 (Nairobi:UNEP, 1992),32. The full text of the London and Copenhagen amendments to the Montreal Protocol on Substances that Deplete Ozone Layer with the Montreal Protocol attached as an appendix can be found at gopher://gopher.law.cornell.edu/00/foreign/fletcher/MONTREAL-1992.txt.

Early work on the suppression of flames by iron pentacarbonyl [2] demonstrated that the introduction of $\text{Fe}(\text{CO})_5$ into a premixed CH_4/air flame lowered the peak concentration of OH and shifted the position of the OH maximum away from the burner surface. Bonne et al. [5] observed that for premixed CH_4/air flames to which small amounts of $\text{Fe}(\text{CO})_5$ were added, the overall reaction rate was inversely proportional to $\text{Fe}(\text{CO})_5$ concentration. However, as $\text{Fe}(\text{CO})_5$ concentrations were increased above a few hundred parts per million the relative effectiveness diminished. Recent investigations by Rumminger et al. [6] of premixed and diffusion CH_4/air flames to which $\text{Fe}(\text{CO})_5$ were added conclude that suppression occurs as a result of H atom removal from the flame by a homogeneous mechanism involving iron oxide scavenging species [7,8]. This is similar to the work of Jensen and Jones [9], who suggest that introduction of $\text{Fe}(\text{CO})_5$ into the flame disturbs the equilibrium balance of the $\text{H}_2\text{O} + \text{H} \ll \text{OH} + \text{H}_2$ reaction, which is one of the principal radical reactions in a hydrocarbon flame.

When iron-containing species are introduced into a flame, highly luminous iron oxide particles are produced [10]. Additionally, Kaufman [11] observed that in the presence of O atoms, $\text{Fe}(\text{CO})_5$ produced fine oxide particles that deposited onto the walls of a reaction tube. The observation of particle formation in a flame by iron-containing species and the formation of particles by $\text{Fe}(\text{CO})_5$ in the presence of O atoms means that a heterogeneous suppression mechanism for $\text{Fe}(\text{CO})_5$ must be considered. However, recent investigations [9] into opposed flow CH_4/air flames to which $\text{Fe}(\text{CO})_5$ was added suggest that particle formation may be indicative of diminishing suppressant effectiveness. Decreasing fire suppression effectiveness with increasing $\text{Fe}(\text{CO})_5$ concentration was attributed to the limiting rate of the homogeneous suppression mechanism, which is determined by the saturation vapor pressure of iron oxide.

The current understanding of the suppression mechanism of $\text{Fe}(\text{CO})_5$ in flames may be summarized as follows. At low additive levels of $\text{Fe}(\text{CO})_5$, radical species responsible for flame propagation are removed by a homogeneous reaction involving iron oxides ($\text{Fe}(\text{O})_x$). As the vapor pressure of the iron oxides approaches saturation, increased addition of $\text{Fe}(\text{CO})_5$ results in formation of iron oxide particles, and a heterogeneous (mixed phase) reaction may become important [5] for depletion of H and OH radicals in the flame system. However, to date there have been no direct measurements of the change in concentration of radical species with increasing addition of $\text{Fe}(\text{CO})_5$ to the flame.

The objective for this work is to experimentally characterize radical species in flames suppressed by $\text{Fe}(\text{CO})_5$ to test currently proposed suppression mechanisms [7]. The experiments presented here were designed to measure the change in OH concentration as extinguishment was approached in reduced pressure, non-premixed, opposed flow, CH_4/air flames suppressed by N_2 , CF_3Br , and $\text{Fe}(\text{CO})_5$. For flames suppressed by CF_3Br , and $\text{Fe}(\text{CO})_5$, we have assumed that the primary mechanism for chemical fire suppression is due to scavenging of the radical species OH and/or H. If the equilibrium condition $\text{H}_2\text{O} + \text{H} \ll \text{OH} + \text{H}_2$ holds throughout the reaction zone, removal of either radical participating in the equilibrium will result in decreased concentration of OH [10]. The flames are examined as they approach extinction using OH emission spectroscopy and OH laser-induced fluorescence (LIF) spectroscopy. Temperatures were measured using Pt/Pt-10%Rh fine wire thermocouples.

EXPERIMENTAL

Figure 1 presents a schematic diagram of the experimental apparatus. The opposed flow burner apparatus is contained within a 200-L combustion chamber, which has been described in detail previously [12]. All flames measured for this work were operated at a pressure of 50 torr. Low pressure opposed flow flames offer an ideal environment to profile combustion intermediate species because the flame zone is expanded. All flames studied consisted of 10L/min synthetic air (79% N₂ + 21% O₂) flowing from the upper duct, and 10L/min of methane flowing upward from the lower duct. The gases are regulated and monitored through a gas handling manifold system constructed from a series of flow controllers (Tylan General). The oxidizer and fuel ducts are separated 3.8 cm and the duct diameter is 7.68 cm. With our flow conditions and flow duct separation, the luminous flame zone is located on the oxidizer side of the stagnation plane and the global strain rate was calculated to be 52 sec⁻¹. For all studies presented here, the inhibitor agents are delivered to the flame zone via the oxidizer duct. It should be noted that Fe(CO)₅ is a liquid at room temperature. The addition of Fe(CO)₅ to the oxidizer stream was accomplished by bubbling argon through a flask containing 25 ml of Fe(CO)₅, which is immersed in a constant temperature bath maintained at 13 °C (at 13 °C the vapor pressure of Fe(CO)₅ is 17.4 torr). The gaseous output of the bubbler apparatus passes through a 5 L/min mass flow meter to monitor the gas stream of argon saturated with Fe(CO)₅ being delivered to the oxidizer stream.

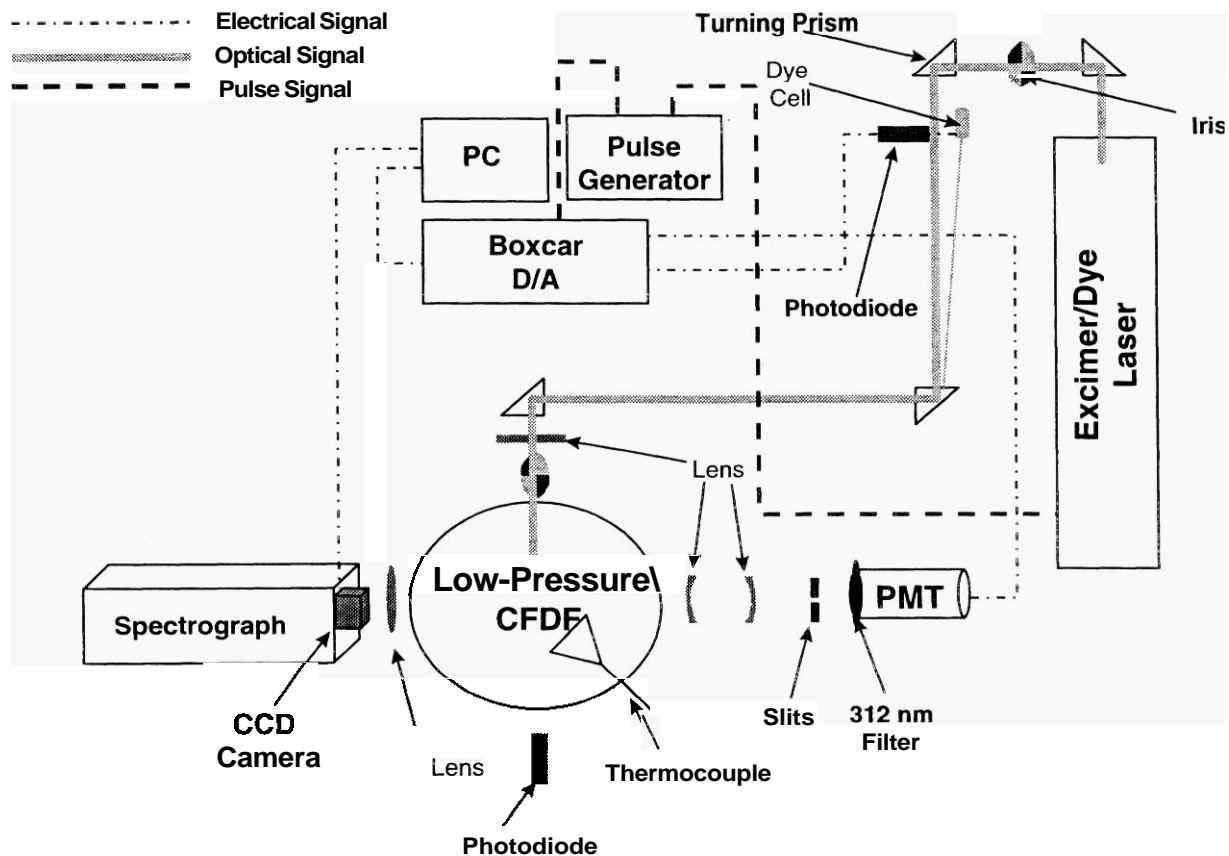


Figure 1. Schematic diagram of the experimental apparatus.

DIAGNOSTICS

Flame emission spectra were measured using a Princeton Instruments ICCD camera (Model 120) coupled to a 0.75 m SPEX spectrograph (Model 1702) with a 1200 gr/mm grating controlled by an external Compudrive. A 50-cm focal length lens collects light from the center of the flame and focuses it onto the entrance slits (0.05 mm) of the spectrograph. The field of view with this optical arrangement was measured to be 1 cm². The ICCD camera, which has an active area of 384 x 576 pixels, was operated in a CW manner, and each image recorded was acquired with 50 total accumulations.

Laser-induced fluorescence excitation spectra in the flame were measured using a Lambda Physik excimer/dye laser system. This system consists of a Lambda Physik Compex 102 XeCl excimer laser, a Scanmate 2 dye laser (Rhodamine 6g) and a Second Harmonic Generator (SHG). The fundamental output of the dye laser (580 nm wavelength) was frequency doubled in the SHG unit with a BBO crystal to around 290 nm. The UV laser radiation was tuned to the peak of the P₂(8.5) transition at 286.566 nm ((1,0) A²S⁺-X²P) [13, 14, 15]. The intensity of this transition is slightly temperature dependent [16], varying by approximately 12% over the range of peak temperatures for the flames studied here (1200 - 1450 K). The UV light output of the SHG unit was focused to the center of the burner chamber using a 50-cm focal length, fused silica lens and had a vertical and horizontal beam waist of 0.4 and 0.5 mm, respectively. Fluorescence was collected at 90 deg to the direction of the excitation laser beam, focused through 0.75 mm horizontal slits to define the collection volume, passed through a band pass filter centered at 312 nm with an 11-nm bandwidth, and detected by photomultiplier tube (PMT) (Phillips Model XP2018B). Laser-induced fluorescence from a cell containing Rhodamine 6g dye was detected by a photodiode to monitor fluctuations in laser power ($\pm 5\%$).

The output signals from the PMT and monitor photodiode were directed to gated integrator/boxcar averagers (SRS Model SR-250) operating in a 10-shot average mode. The boxcar gate widths were set to 3 ns. The trigger pulses to the excimer laser and boxcars were supplied by a digital delay pulse generator (SRS Model DG535) at a rate of 10 Hz. Spatially resolved OH LIF profiles are measured by tuning the excitation laser to the peak of the P₂(8.5) transition and, with the beam location fixed, vertically translating the burner assembly.

The combustion chamber has ports at 45 deg relative to the optical windows that allow access for the thermocouple apparatus. Temperatures were measured using a 0.2 mm diameter Pt/Pt-10% Rh fine wire thermocouple, which were coated with magnesium oxide prior to flame measurements to decrease catalytic effects [13]. All experimental temperature data reported here are uncorrected for emissivity.

RESULTS

For opposed flow CH₄/air flames at a total pressure of 50 torr and a strain rate of 52 sec⁻¹, agent concentrations at extinction were 9426 ppm for N₂, 3735 ppm for CF₃Br, and 451 ppm for Fe(CO)₅. The average uncertainty in agent concentration at extinction due to measurement variance was determined to one standard deviation of 6, 18, and 17 percent for N₂, CF₃Br, and Fe(CO)₅ respectively. Numerical calculations of extinction concentrations for CF₃Br and Fe(CO)₅ were 4000 and 271 ppm, respectively [17]. The numerical calculations of Fe(CO)₅

concentration at extinction for the 50 torr opposed flow flames assumed a homogenous mechanism.

It should be noted that addition of N_2 or CF_3Br , to the 50 torr CH_4 /air flame does not significantly alter the physical appearance of the flame, which is a cylindrical, flat blue flame. Addition of $Fe(CO)_5$ to the flame causes an orange/yellow luminous region to appear above the blue luminous zone. As the flame approaches extinction, the blue luminous zone gradually disappears and the flame assumes a uniform bright orange/yellow color. The orange/yellow luminosity in the $Fe(CO)_5$ inhibited flame is believed to be caused by iron oxide emission.

EMISSION SPECTROSCOPY

Figure 2 shows an OH emission image measured along the centerline of an opposed flow methane/air unsuppressed flame. To construct a graph of OH emission versus position in the flame, the pixel intensity corresponding to a given height in the flame (spatial resolution approximately 0.026 mm) was summed over the wavelength range corresponding to the R1, R2 OH rotational lines near a wavelength of 312 nm. These rotational lines were chosen because they are free from interferences from Fe emission lines, which appear throughout the OH spectral region in CH_4 /air flames suppressed by $Fe(CO)_5$.

Figure 3 displays representative, spatially resolved OH emission profiles for each of the flames examined for this study. Each profile has been normalized to the peak intensity of the OH emission profile measured in an unsuppressed flame. The suppressant concentrations are 78%, 66%, and 55% of the concentration required for extinguishment by N_2 , CF_3Br , and $Fe(CO)_5$, respectively. The results show that for the flames to which $Fe(CO)_5$, CF_3Br , or N_2 have been added, the greatest OH emission intensity is for the flame to which CF_3Br has been added, followed by the flame to which N_2 has been added. The flame to which $Fe(CO)_5$ has been added shows the smallest OH emission intensity. The difference between the N_2 and CF_3Br doped flames is not statistically significant since the profiles have a 1s error of 10%, thus they are essentially the same.

Ground-state populations and temperatures calculated from OH emission in flames using a Boltzman distribution can be misleading because nascent OH may not be in thermal equilibrium with other combustion gases. Thus, relating OH flame emission intensity to total OH concentration may be misleading. Nevertheless, the results presented here qualitatively show that as extinguishment is approached, the OH emission from the flame to which $Fe(CO)_5$ has been added is significantly less than that for flames to which either N_2 or CF_3Br has been added (which are in greater concentration percentages than $Fe(CO)_5$).

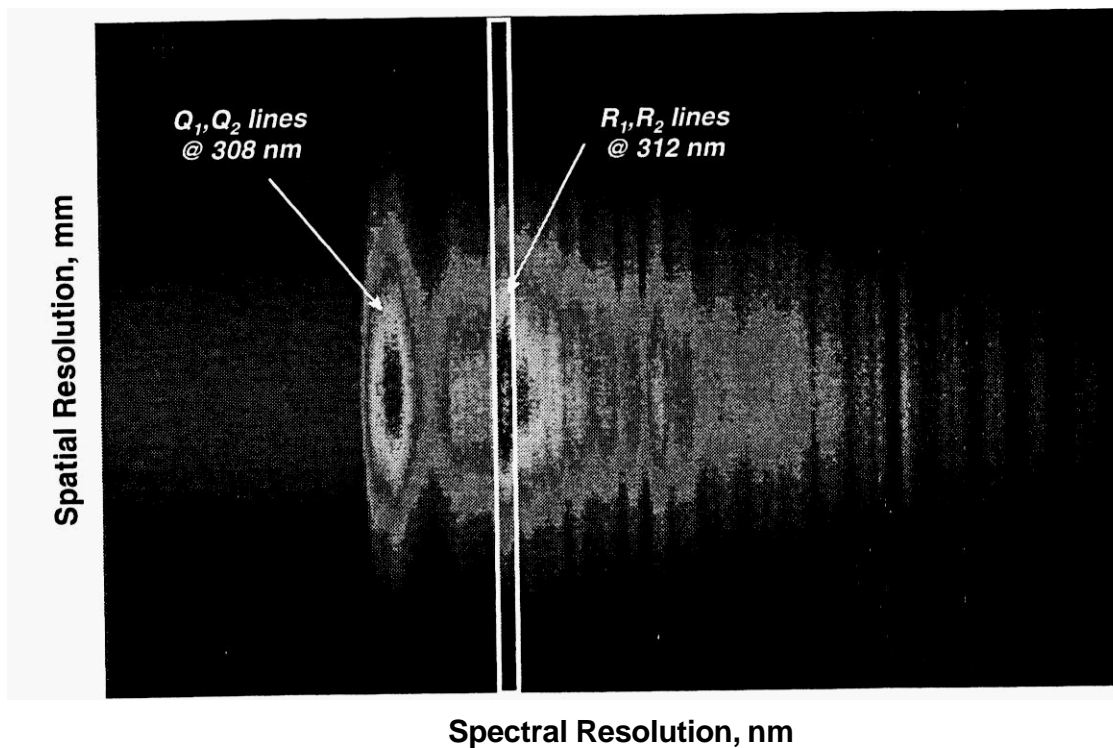


Figure 2. Representative OH emission image from the unsuppressed flame.

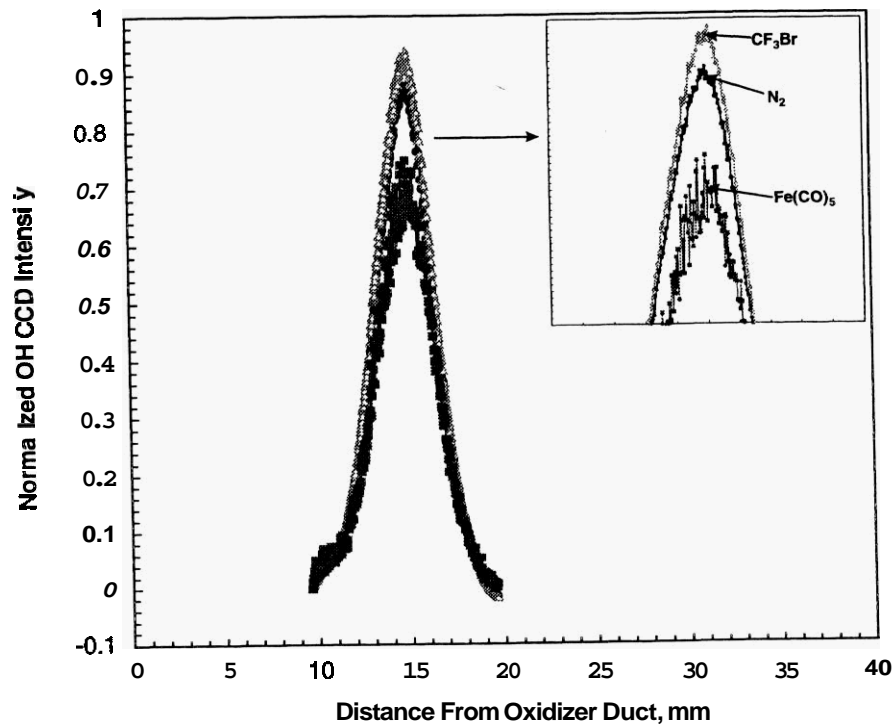


Figure 3. OH emission profiles from flames containing 7412 ppm of N_2 (\bullet), 2493 ppm of CF_3Br (Δ), and 236 ppm of $Fe(CO)_5$ (\blacksquare).

LASER-INDUCED FLUORESCENCE

Figure 4 shows relative OH LIF profiles measured in 50-torr opposed flow CH₄/air flames to which Fe(CO)₅, CF₃Br, or N₂ has been added. The suppressant concentrations are 78%, 66%, and 55% of the concentration required for extinguishment by N₂, CF₃Br, and Fe(CO)₅, respectively. The data shown have been normalized to the peak intensity of the OH LIF profile measured in an un-suppressed flame. Figure 4 illustrates that for the suppressed flames examined here, the flame to which N₂ has been added has the highest OH LIF intensity followed by the flame to which CF₃Br has been added. The OH LIF measured in the flame to which Fe(CO)₅ has been added has the lowest intensity of the three, in agreement with emission measurements (Figure 3).

Figure 5 presents the normalized OH LIF peak intensities for each agent studied versus the amount of suppressant added to the flame. The data here show the relative effectiveness of each agent: iron pentacarbonyl is the most effective agent on a concentration basis because it extinguishes the flame when added in the least amount relative to CF₃Br or N₂.

Radiative cooling effects due to iron oxide particles produced in flames to which Fe(CO)₅ has been added may contribute to the enhanced fire suppression relative to CF₃Br. In hydrocarbon/air flame systems that produce carbon particulate, as the concentration of soot increases, OH radical concentrations and temperatures decrease [18,19,20]. Figure 6 shows thermocouple temperature profiles (uncorrected for thermal emission) measured in flames studied here at suppressant levels of 71% for N₂, 40% for CF₃Br, and 21% for Fe(CO)₅. Temperature profiles of flames to which CF₃Br or N₂ have been added are not statistically different from those measured in an un-suppressed flame. The temperature profile for the flame to which Fe(CO)₅ has been added shows a 100 K decrease in the peak flame temperature. Temperature measurements at higher Fe(CO)₅ concentrations show continuing decreases in temperature, but are subject to greater uncertainty due to particulate coating of the thermocouple wire. Similar decreases in flame temperatures have been observed by Brabson et al. [4] in studies of low-pressure premixed flames suppressed by Fe(CO)₅. The enhanced fire suppression effectiveness of Fe(CO)₅ relative to CF₃Br may occur partly because of the flame temperature lowering capabilities of Fe(CO)₅.

CONCLUSIONS

The experimental results presented here show for the first time the change in OH concentration as fire extinguishment is approached in low pressure, non-premixed, methanellair diffusion flames. For the flames suppressed by Fe(CO)₅ and CF₃Br, the decrease in the OH population is proportional to the amount of suppressant added. Evidence is also provided that suggests that a decrease in local flame temperatures could enhance Fe(CO)₅ suppression effectiveness.

ACKNOWLEDGMENTS

The authors would like to thank E. Lancaster for his help with the experimental arrangements. Much of the OH LIF data analysis was aided through the generous guidance of A. Kotlar. Finally R. Skaggs was financially supported by an American Society for Engineering Education Postdoctoral Fellowship.

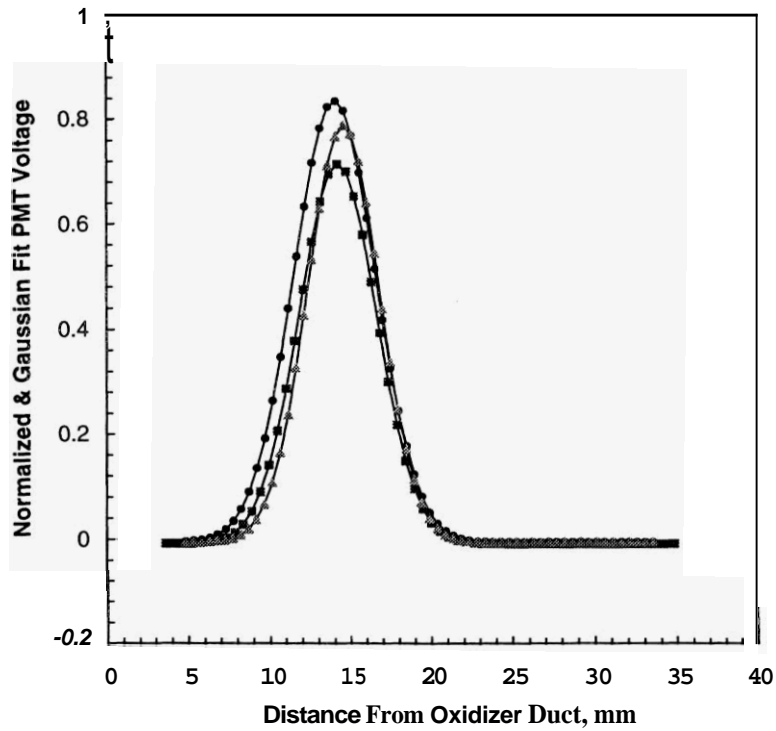


Figure 4. LIF OH profiles collected from flames containing 7412 ppm of N_2 (●), 2493 ppm of CF_3Br (▲), and 236 ppm of $Fe(CO)_5$ (■).

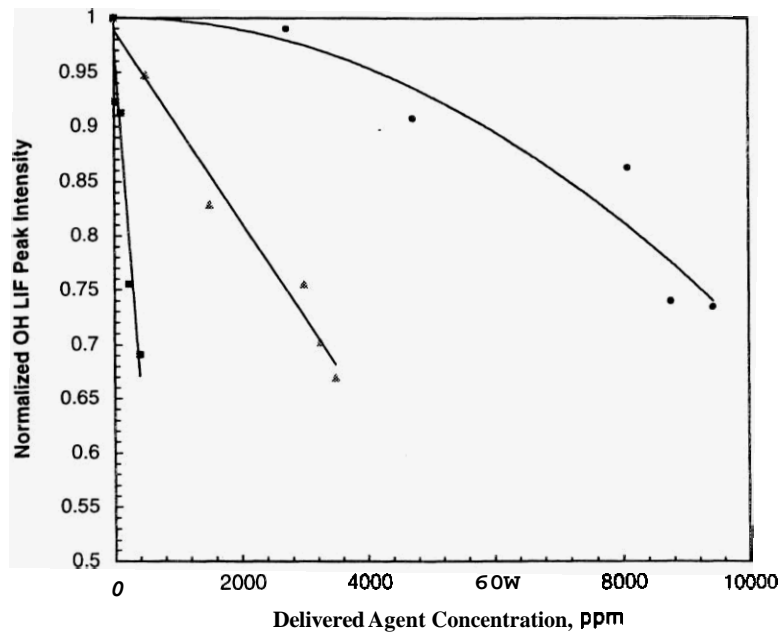


Figure 5. Normalized OH LIF profile peaks versus agent delivery concentrations to extinguishment. The (●) are the N_2 data, the (▲) are the CF_3Br data, and the (■) are the $Fe(CO)_5$ data.

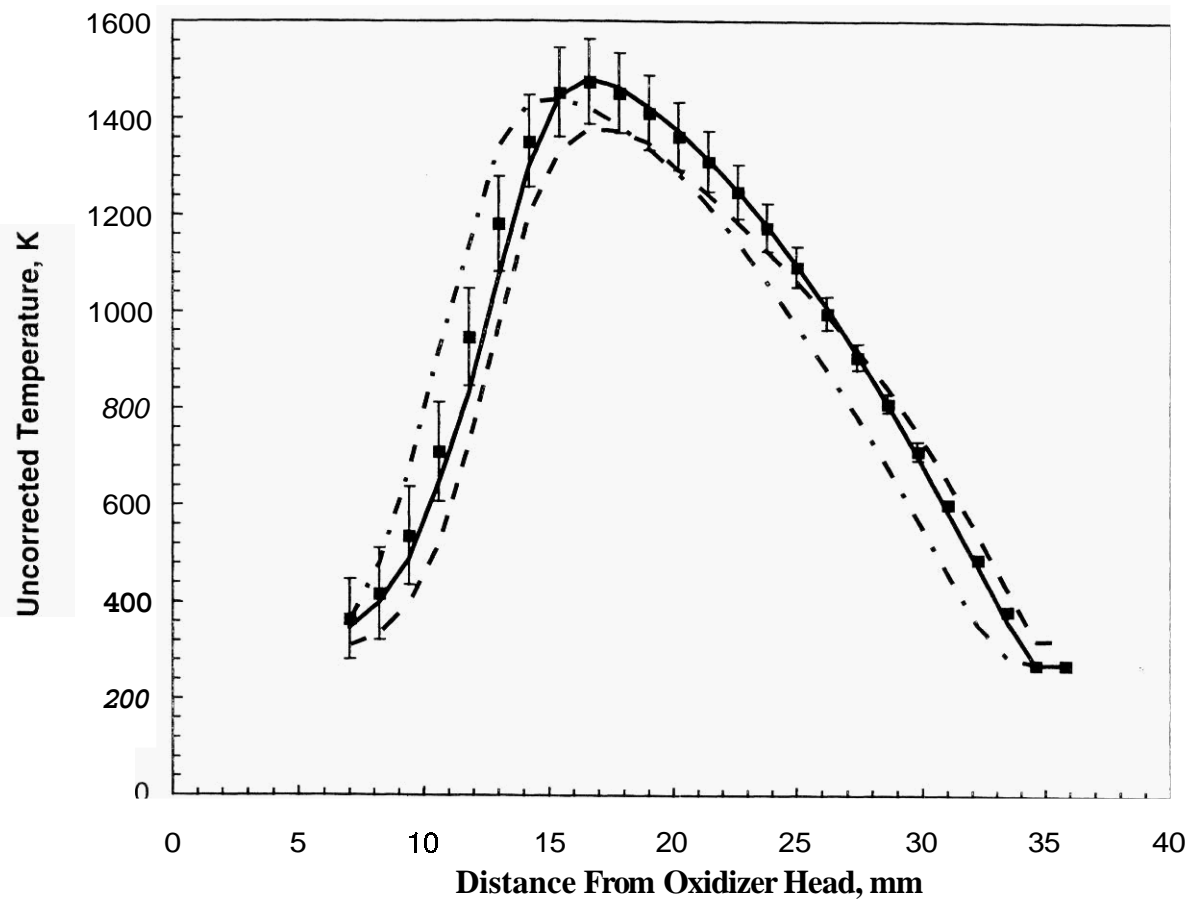


Figure 6. Uncorrected thermocouple temperature profiles collected each studied flames. The flames seeded with N₂ (dot-dashed line), CF₃Br (solid line), Fe(CO)₅ (dashed line) were at concentrations of 6739, 1497, 98 ppn respectively. The (■) symbols represent a characteristic unsuppressed flame temperature profile.

REFERENCES

1. Lask, G., and Wagner, H. G., *Eighth Symposium(International) on Combustion*, The Combustion Institute, Williams and Wilkens, Baltimore, MD, 1962, pp.432-438.
2. Bonne, U., Jost, W., and Wagner, H.G., *Fire Research Abstracts and Reviews* 4: 6-18 (1962).
3. Brabson, G.D., Walters, E.A., Gennuso, A.R., Owen, J.P., and Tapscott, R.E., "Molecular Beam Mass Spectrometry of Low-Pressure Flames Seeded with Iron Pentacarbonyl," submitted *J. Phys. Chem.*, 1998.
4. Pitts, W.M., Nyden, M.R., Gann, R.G., Mallard, W. G., and Tsang, W., in *Construction of an Exploratory List of Chemicals to Initiate the Search for Halon Alternatives*, NIST Technical Note 1279, US Department of Commerce, Chapter 3: Section J., pp. 73-74.
5. Jost, W., Bonne, U., and Wagner, H.G., *Chemical and Engineering News*, vol. 39, p. 76, 11 September 1961.
6. Rumminger, M.D., Reinelt, D., Babushok, and Linteris, G.T., submitted to *Combustion and Flame*, 1997.
7. Reinelt, D., and Linteris, G.T., *Twenty-Sixth Symposium (International) on Combustion*, The Combustion Institute, Pittsburgh, PA, 1996, 1421-1428.
8. Reinelt, D., Linteris, G.T., and Babushok, V., *Chemical and Physical Processes in Combustion*, 1996, 273-276.
9. Jensen, D.E., and Jones, G.A., *J. Chem. Phys.* 60(9):3421-3425 (1974).
10. Hastie, J.W., in *High Temperature Vapors*, Academic Press, New York, 1975, pp. 335-357.
11. Kaufman, F., *Proc. Roy. Soc. (London)* A247, 123-139 (1958).
12. Daniel, R.G., McNesby, K.L., Skaggs, R.R., Saguear, P., and Miziolek, A.W., *Proceedings of the 1997 JANNAF Combustion Subcommittee Meeting*, West Palm Beach, FL.
13. Chidsey, I.L., and Crosley, D.R., *J Quant. Spectrosc. Radiat. Transfer, Vol. 23*: 187-199 (1980).
14. Dieke, G.H., and Croswhite, H.M., *J Quant. Spectrosc. Radiat. Transf.* 2: 97-199 (1962).
15. Kottlar, A., Personal Communication (1998).
16. Eckbreth, A.C., in *Laser Diagnostics for Combustion Temperatures and Species*, Abacus Press, Cambridge Mass., (1988).
17. Smooke, M.D. Personal Communication (1997).
18. Puri, R. and Santoro, R.J., *Fire Safety Science, Proceedings of the Third International Symposium*, 1991, pp. 595-604.
19. Skaggs, R.R. and Miller, J.H., *Combust. and Flame*, 100:430-439 (1995).
20. Skaggs, R.R. and Miller, J.H., *Twenty-Sixth Symposium (International) on Combustion*, 1996, 1181-1188.